MESOCARP ULTRASTRUCTURE AND MITOCHONDRIAL ENZYME ACTIVITY IN GRAPE BERRY DURING CELLULAR VIABILITY LOSS

EDUARDO MONTEIRO

UNIVERSIDADE ESTADUAL DO NORTE FLUMINENSE DARCY RIBEIRO

CAMPOS DOS GOYTACAZES - RJ

MARCH - 2023

MESOCARP ULTRASTRUCTURE AND MITOCHONDRIAL ENZYME ACTIVITY IN GRAPE BERRY DURING CELLULAR VIABILITY LOSS

EDUARDO MONTEIRO

"Thesis presented to the Centro de Ciências e Tecnologias Agropecuárias from Universidade Estadual do Norte Fluminense Darcy Ribeiro, as part of the requirements for obtaining the Master's title in Plant Science"

Advisor: Prof. Ricardo Bressan-Smith

CAMPOS DOS GOYTACAZES - RJ

MARCH - 2023

MESOCARP ULTRASTRUCTURE AND MITOCHONDRIAL ENZYME ACTIVITY IN GRAPE BERRY DURING CELLULAR VIABILITY LOSS

EDUARDO MONTEIRO

"Thesis presented to the Centro de Ciências e Tecnologias Agropecuárias from Universidade Estadual do Norte Fluminense Darcy Ribeiro, as part of the requirements for obtaining the Master's title in Plant Science"

Approved on 1st March, 2023

Examination Committee:

_____

Antônia Elenir Amâncio Oliveira - (D.Sc. Biociências e Biotecnologia) - UENF

_____

Olfa Zarrouk - (D.Sc. Agricultural System, Forest and Nutrition Systems) - ULisboa

_____

Stefania Savoi - (D.Sc. Agricultural Science and Biotechnology) - UniTo

_____

Ricardo Bressan-Smith - (D.Sc. Produção Vegetal) - UENF
(Adviser)

TABLE OF CONTENTS

ABSTRACT

MONTEIRO, Eduardo; M. Sc; Universidade Estadual do Norte Fluminense Darcy Ribeiro; 03/2023; Mesocarp Ultrastructure and Mitochondrial Enzyme Activity in Grape Berry During Cellular Viability Loss; Ricardo Bressan-Smith, Antônia Elenir Amâncio Oliveira, Olfa Zarrouk, Stefania Savoi.

Xylematic connections between fleshy fruits and the mother plant are disconnected at the ripening of grapes berries, resulting in a physiological event known as "hydraulic isolation". Our research group found that this occurs in *cv.* 'Niagara Rosada' (NR) just after the *veraison*, concomitantly with the loss of the viability of the mesocarp cells. To test the hypothesis that mesocarp cells undergo loss of cell compartmentation and vitality but not cell death, we were able to isolate intact mitochondria at different stages in two consecutive years from the mesocarp of NR. We determined that malate dehydrogenase and succinate dehydrogenase enzymes presented lower activities later in ripening, while fumarate remained constant. Cells from the outer mesocarp changed over ripening, exhibiting large spaces among them, while the intercellular cell wall became less electron-dense. The combination of enzymatic respiratory activity, mitochondria integrity and ultrastructure proved to be effective for testing the viability of berry mesocarp. The present data indicate that the loss of berry mesocarp integrity was not associated with cell death.

RESUMO

As conexões xilemáticas entre frutos carnosos e a planta-mãe se desconectam com o amadurecimento do fruto, levando ao "isolamento hidráulico". Nosso grupo de pesquisa tem demonstrado que esse evento ocorre em bagas da variedade 'Niagara Rosada' (NR) logo após o *veraison*, levando à chamada morte celular do mesocarpo. Neste trabalho será testado a hipótese de que as células do mesocarpo perdem compartimentação e vitalidade celular, sem a ocorrência de morte celular, enquanto mantem membranas celulares e mitocondriais intactas. Para confirmar essa hipótese, mitocôndrias intactas foram isoladas do mesocarpo de NR em diferentes estágios em dois anos consecutivos. Foi determinado enzimaticamente que as enzimas malato desidrogenase e succinato desidrogenase apresentaram menor atividade com o amadurecimento, enquanto a fumarase mantém a atividade constante. O espaço intercelular no mesocarpo aumentou enquanto a parede celular tornou-se menos eletrodensa com o amadurecimento. A combinação de atividades enzimáticas relacionadas à respiração, integridade mitocondrial e ultraestrutura foi eficaz para testar a viabilidade do mesocarpo da baga. Os dados aqui apresentados indicam que a perda da integridade do mesocarpo da baga não foi associada à morte celular.

1. INTRODUCTION

Researchers shared the consensus that the xylem connections between the fleshy fruit and the mother plant become physically disrupted as the fruit ripens (Greenspan et al., 1994; Delrot et al., 2001), and that a generalized loss of cell content to the apoplast leads to loss of cell viability, firmness and turgor pressure (*P*) (Lang and Düring, 1991; Dreier et al., 1998). However, such statements seem to be more intricate. Xylem connection to the berry remains physically intact and without occlusion (Bondada et al., 2005, Keller et al., 2006, Chatelet et al., 2008a; 2008b) until post-*veraison*, where polysaccharide-like material (i.e. gels or solutes) were found to obstruct the pedicel xylem (Choat et al., 2009; Knipfer et al., 2015).

Grape berry cell membranes are maintained viable with positive *P* values (Thomas et al., 2006), promoting substantial integrity and cell viability throughout the development (Krasnow et al., 2008). Xylem hydraulic conductance in berries appears to be associated with cell viability status. Fuentes et al. (2010) analysed several varieties and identified three groups supporting the hypotheses of a mechanistic link between tissue vitality and water relations of the berry: the group with the lowest hydraulic conductance sustained lower cell vitality. The loss of cell vitality can be interpreted as leakage in the plasmatic membrane, even if their appearance remains structurally intact (Caravia et al., 2015).

1

Our research group found evidence of earlier membrane integrity loss in 'Niagara Rosada' berries (NR) (Lerin, 2016; Bezerra, 2018) when compared to varieties such as Chardonnay, Thompson Seedless, and Shiraz (Tilbrook and Tyerman, 2008). Moreover, Lerin (2016) identified a loss of xylem functionality just after veraison. Regardless, cellular respiratory processes were not consistently studied along with cell viability. One of the few pieces of evidence was the dehydrogenase activity at later developmental stages in the mesocarp of NR (Bezerra, 2018). Another evidence was the decrease of the berry internal O_2 concentration throughout the development, with a high correlation with mesocarp cell death in *cv*. Shiraz (Xiao et al., 2018a; 2018b). We were suspicious that cell death was not occurring in NR post-*veraison*, even with the occurrence of membrane integrity loss. Therefore, we propose to demonstrate that NR mesocarp cells maintain respiratory activity, irrespective of undergoing loss of compartmentation and vitality, or even cell death.

2. BIBLIOGRAPHIC REVIEW

2.1 *Vitis*

Plants from the genus *Vitis* are perennial vines or shrubs with tendril-bearing shoots (Keller, 2015) with deciduous leaves (Iland et al., 2011). It is considered a temperate deciduous plant, but it can adapt to different climates (Sentelhas, 1998). Consequently, viticulture is also distributed in the Tropics worldwide. In Brazil, the production is in the South (mostly wine grapes), and Southeast and Northeast regions (mostly table grapes). The vines are generally undemanding regarding the cold, and when cultivated in a hot and dry climate, with high light intensity and low rainfall rates, it presents different phenologic stages from that observed in temperate and subtropical climate regions (Pires, 1998). For example, viticulturists can carry out pruning at any time of the year as long as the buds are mature. The pruning season marks the beginning of the vine phenological cycle conditioned by climatic factors prevailing during that period. The Modified Eichhorn-Lorenz System (Coombe, 1995) divides the wine cycle into 47 stages and is a tool to identify major and/or precisely defined stages for the correct classification of grapevine growth stages.

The inflorescence is a panicle with a varying structure (Pratt, 1971; May, 2000). In general, the grapevine varieties cultivated are hermaphrodite flowers in which self-fertilization occurs (Oberle, 1938). The bunch or cluster is composed of a peduncle, rachis (or stalk), pedicel and flowers that when fertilized will turn on berries consisting of skin (formed by cuticle, the epidermis, and the hypodermis), fleshy mesocarp (formed by polygonal cells), and seeds (formed by cuticle, an epidermis, and envelopes covering the albumen and the embryo). The number of berries decreases along the acropetal sequence of the rachis (because of the panicle structure) and cluster compactness depends on the length of the pedicels, forming either spread-out or compacted grapes. The basal portion of the axial and seed vascular bundles (distinct packets of xylem and phloem cells) in grapes are designated as "brush", through which water and solutes are supplied to the berry. The brush is connected to the mother plant by the receptacle in the pedicel (May, 2000; Ribéreau-Gayon et al., 2006; Jackson, 2008).

2.2 Berry Growth

The development of the grape berry follows the same pattern as other fleshy fruits, being represented by a double sigmoid growth curve with three distinct phases (Coombe, 1976): two fast-growing phases separated by a period of slow growth. However, the boundaries between these phases are determined arbitrarily and exhibit logical difficulties. Phase I is marked by intense metabolic activity and cellular replication and is characterized by elevated respiratory rate and rapid accumulation of acids. In Phase II, the berry undergoes a period of little or no growth. In the transition to Phase III, substantial changes in terms of the physiology of the grape take place, the *veraison*, which is considered the beginning of the ripening phase. Phase III is the second growth phase and corresponds to berry maturation. In this phase, the berry softens, the respiratory rates decrease, sugar content increases along with acid catabolism, and the colour develops. At maturity, berry size depends largely on these physiological processes but is also dependent on the number of cells per fruit (Ribéreau-Gayon et al., 2006).

The onset of *veraison* is marked by berry softening (which can be measured as deformability), coinciding with the accumulation of sugars and taking

place several days before the colour change (Coombe, 1976; Keller, 2015). In a variety of fruits, softening is largely attributed to the action of enzymes that modify the cell wall (Goulao et al., 2008). Changes in cell wall polysaccharides during grape ripening suggest a limited number of enzymes that play an important role in the softening process, such as endo- or exohydrolases, pectin methylesterase, and endo-polygalacturonase (Nunan et al., 1998). While berry softening has shown to be a consequence of cell wall structure modification, berry firmness is strongly associated with turgor (*P*) pressure of mesocarp cells (Thomas et al., 2008; Wada et al., 2008; Matthews et al., 2009). Similar observations of *P* during softening in tomato (*Solanum esculentum*) (Shackel et al., 1991; Saladié et al., 2007) and apple (*Malus* spp.) (Tong et al., 1999) indicate that decreases in *P* can serve as a primary softening mechanism, which essentially precedes all other physiological events that occur during or around the *veraison* period (Matthews and Shackel, 2005; Thomas et al., 2006; 2008).

Historically, *veraison* is classified as the colour change of the berry (*véraison* comes from French for "painter"). Anthocyanin concentration is the main responsible for coloured berries. Synthesized in the flavonoid pathway, which leads to the synthesis of other compounds such as flavonols, flavan-3-ols, and proanthocyanidins, these molecules are classified as phenolics and are good antioxidants, and contribute to grape flavour and aroma. Flavonoids can be found in other places like seeds and stems, but after synthesis in the cytosol, anthocyanins are predominantly stored in the vacuole of the berry epidermis and first hypodermal layer. The specific colour of white grape cultivars comes from other molecules such as carotenoids, xanthophylls, and flavonols like quercetin (Jackson, 2008; Castellarin et al., 2012; Keller, 2015). Anthocyanins are regulated in grape skins through a variety of environmental stimuli such as developmental signals, environmental stresses (light, temperature, irrigation/water status, etc.), and plant growth regulators (Boss and Davies, 2009).

2.3 Grape Hydraulic Isolation and Mesocarp Cell Viability

Especially in fruits with fleshy pulp, water relations are crucial because of a common element in fruit development: the accumulation of high solute concentration. Among these, particularly sugars must be retained in the cells, without causing excessive cellular turgor, which could lead to "cracking", or retained in the apoplast, without being relocated to the vegetative tissues of the plant (Lang and Thorpe, 1988). Over the past two decades, the consensus among researchers has shown that the xylem connections between the fleshy fruit and the mother plant become physically disrupted as the fruit ripens (Greenspan et al., 1994; Delrot et al., 2001). However, evidence considered that the xylem pathway to the berry remained physically intact and without occlusion (Bondada et al., 2005; Keller et al., 2006; Chatelet et al., 2008a; 2008b) until after *veraison*, where polysaccharide-like material, gels or solutes, has been reported in the pedicel xylem (Choat et al., 2009; Knipfer et al., 2015). Even with Knipfer et al. (2015) founding blockages in vessel elements and Choat et al. (2009) founding deposition of gels or solutes in many receptacle xylem conduits, their presence does not completely cease the water flux and sometimes occurs too late in development to explain the decline in xylem flow that occurs before their blockages. Yet, the amount of water supplied by the xylem to the berry decreases, and the predominant water pathway supply shifts from the xylem to the phloem at *veraison* (Matthews and Shackel, 2005). This shift coincides with the switch of phloem unloading from a symplastic to an apoplastic pathway (Zhang et al., 2006). The resulting presence of solutes in the fruit apoplast (Keller and Shrestha, 2014) increases its osmotic pressure (Wada et al., 2008; Keller et al., 2015), enhancing osmotic water outflow from the phloem, 'hydraulic buffering' the xylem, which helps to explain the decline in its inflow. The xylem hydraulic conductance is reduced depending on the variety (Tyerman et al., 2004; Tilbrook and Tyerman, 2009), or continues in post-*veraison* berries (Bondada et al., 2005) but its pressure changes from negative to positive during *veraison*, causing xylem backflow, which may be necessary to the normal grape ripening (including, or not, berry transpiration) (Keller, 2015; Zhang et al., 2017). However, Carlomagno et al. (2018) considered that the vine gradually loses the ability to deliver water to the berries via pedicel during ripening, where the xylematic back-flow is active in the pre-*veraison* but not in the post-*veraison* berries. However, they do not clarify whether this is due to a vessel/tracheid breakage or not.

The hypothesis "that apoplast:symplast compartmentation substantially breaks down around the time of onset of ripening in grape berries and that this, apparently, is a normal and integral part of berry development", suggests a generalized loss of cell content to the apoplast, leading to loss of cell viability, firmness, and P (Lang and Düring, 1991; Dreier et al., 1998). The loss of membrane integrity and compartmentation is acknowledged as a normal part of the development of grape berries, indicating the end of homeostasis and the onset of mesocarp cell death (Noodén, 2003). However, Thomas et al. (2006) found that grape berry cell membranes remain viable with positive P values, exhibiting functional membranes after apparent hydraulic isolation at the beginning of maturation. Following this, Krasnow et al. (2008) pointed to the substantial maintenance of membrane integrity and cell viability in berries throughout development, and Fontes et al. (2011) demonstrated intact plasma membrane in protoplasts isolated from fully ripened grape mesocarp cells. Tilbrook and Tyerman (2008) demonstrated varietal differences in the loss of cell vitality and linked it to changes in osmotic behaviour, while Fuentes et al. (2010) linked it to the occurrence of berry shrivel. Analysing 22 varieties, they identified three groups that reflect different xylem hydraulic conductances of the berries, showing how the water relationship might be linked with membrane vitality: the group with the lowest conductance was the one with lower cell vitality. However, weather variations (heat waves and water stress) would impact the degree of loss in cell vitality (Bonada et al., 2013a; 2013b; Xiao et al., 2018a; Clarke and Rogiers, 2019).

Our research group found evidence of membrane integrity loss in 'Niagara Rosada' berries (NR) in an early stage (Lerin, 2016; Bezerra, 2018) when compared to varieties such as Chardonnay, Thompson Seedless, and Shiraz (Tilbrook and Tyerman, 2008) as well loss of xylem functionality (Lerin, 2016). Dye staining via fluorescein diacetate (FDA) to access cellular viability/vitality through membrane integrity was the only technique employed until the research by Caravia et al. (2015). By using electrical impedance, measured by passing an alternating current of various frequencies across the berry tissues, they concluded that cell membranes, although becoming leaky, may remain intact, hence: "*It remains to be determined how decreased vitality is manifested in the berry as cell*

membranes appear to remain structurally intact despite the high probability they become leaky".

Most studies with loss of membrane integrity and cell viability did not assess the cellular respiratory process. For Xiao et al. (2018a; 2018b), berry respiration analysed by O_2 uptake indicated that grape internal O_2 declined during fruit development, with a high correlation with the profile of mesocarp cell death observed. In addition, ethanol was found in high concentrations in Chardonnay berries as a result of a shift from oxidative phosphorylation to fermentation. It is known that ethanol alters the respiratory quotient (RQ = CO_2 released/O_2 consumed) of grape mitochondria and uncouples oxidative phosphorylation (Romieu et al., 1992). Given the importance of how the metabolic pathways persist even with the high loss of cell viability in NR berries, our group has demonstrated evidence of dehydrogenase activity, enzymes associated with respiratory activity, at later developmental stages in the mesocarp, even with the loss of cell viability (Bezerra, 2018).

2.4 Grape Respiration

Grape berries are non-climacteric fruits, meaning that respiration burst and accumulation of ethylene are not found at the ripening stage (Coombe and Hale, 1973). However, there is evidence demonstrating regulation by ethylene (Tesniere et al., 2004). In grapes, respiration follows the same three simple processes: glycolysis, tricarboxylic acid (TCA) cycle, and oxidative phosphorylation by electron transport chain (ETC). Glucose and fructose, the substrates for respiration, are initially photosynthesized *in situ*. At Phase III, sucrose is readily translocated within the phloem from leaves located on the same side of the shoot of the berry cluster. Firstly, sucrose is hydrolyzed into glucose and fructose. In pre-*veraison* berries, the proportion of glucose is usually higher and during ripening, the glucose/fructose ratio falls. Despite inhibition in glycolysis rate (Ruffner and Hawker, 1977), it is important to note that the glycolytic pathway remains functional to some extent in the mesocarp during ripening in grapes (Famiani et al., 2000; Terrier and Romieu, 2001). At this point, malic acid is promptly imported from the vacuole to be used in energy production. Organic acids, the secondary product of sugar metabolism, being 90% tartaric and malic acid, are produced *in*

Mesocarp Cell Viability

Xylem Influx
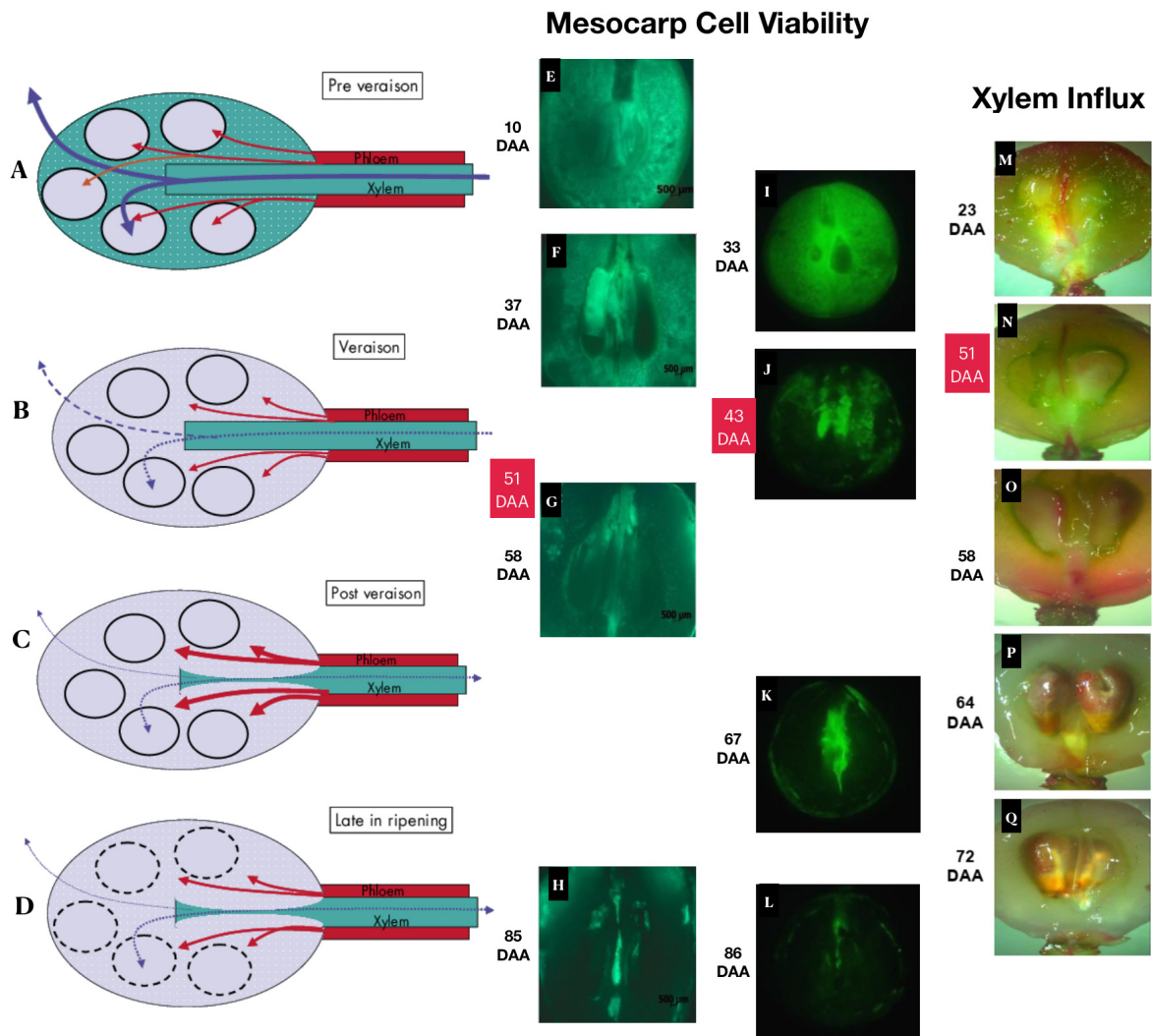
Figure 1. Changes in xylem, phloem and transpiration components of berry water balance during four stages in ripening (A, B, C, D), Fluorescein diacetate dye fluorescence images accessing 'Niagara Rosada' mesocarp cell viability (E, F, G, H, I, J, K, L) and passive infusion of acid fuchsin dye to access 'Niagara Rosada' xylem influx (M, N, O, P, Q). DAA: Day After Anthesis. A, B, C and D adapted from Tilbrook and Tyerman (2006); E, F, G, H, M, N, O, P and Q adapted from Lerin (2016) and I, J, K, L adapted from Bezerra (2018).

situ and stored at the vacuole. Malic acid can be respired, giving rise to glucose by gluconeogenesis pathway, or fermented (Ruffner and Hawker, 1977; Terrier and Romieu, 2001.) When respired, the oxidation of malate elevates the RQ (Peynaud and Ribereau-Gayon, 1971). Famiani et al. (2014) demonstrated that malate is only quantitatively responsible for the increase of the RQ in exocarp for a short time at *veraison*. Other processes such as ethanolic fermentation (Romieu et al., 1992) and the use of NADH were found to be responsible for the increase in the RQ. Famiani et al. (2016) considered that most of the malate is not used by gluconeogenesis in the grape pericarp. At the onset of ripening, malate is discharged from the vacuole and readily respired (Shahood et al., 2020). The

efflux of malic acid to the cytoplasm requires sugar to be pumped back to the vacuole, consuming ATP, shifting respiration back to sugars, and inducing an aerobic fermentative pathway. After the production of chemical energy and reducing equivalents by TCA, adenosine triphosphate (ATP) is produced by F1-ATPase after the ETC (Ribéreau-Gayon et al., 2006; Ford, 2012; Keller, 2015).

The respiration process takes place in the cytosol and mitochondria. It is known that mitochondrial integrity is often maintained until late in the senescence process (Noodén, 2003). Tian et al. (2013) considered that reactive oxygen species (ROS [such as H_2O_2, OH, and O_2]) mediated mitochondrial impairment, is one of the major factors associated with senescence. Indeed, fruit senescence requires an increase in ROS production. As postulated by Pilati et al. (2014), harmless accumulation of ROS at the cytosol and chloroplast of the skin is, at a definite developmental stage, the onset of grape berry ripening. ROS can damage lipids, which may trigger membrane deterioration (Thompson, 1998), besides the damage to proteins and DNA. In plants, the ETC is an important site of ROS production (Møller, 2001). MDH and aconitase from TCA are some of the enzymes affected by ROS oxidative damage in apple (Quin et al., 2009). In peach, activities from catalase (CAT), succinate dehydrogenase (SDH), and cytochrome c oxidase (CCO) were relatively lower when the rate of ROS production reached a maximum (Juan et al., 2010). Mitochondrial enzymatic systems like CAT activity, ascorbate/ glutathione cycle, and others are possibly involved in ROS detoxification (Møller, 2001; Wu et al., 2016). Sarry et al. (2004) considered that stress-related protein in the mesocarp of different grape varieties includes defence towards ROS scavenging systems, Pilati et al. (2014) demonstrated CAT activity as a ROS scavenger in skin samples and our group observed higher CAT activity in mesocarp at *veraison* (Bezerra, 2018). ROS are nowadays more correctly described as dynamic and powerful providing intrinsic signalling to many developmental processes and responses to the environment (Noctor and Foyer, 2016), being described as the onset of berry grape ripening (Pilati et al., 2014).

3. MATERIAL AND METHODS

3.1 Plant Material

Berries from the cv. Niagara Rosada (somatic mutation from cv. Niagara, *V. labrusca* 'Concord' x 'Cassady' (*V. labrusca* X *V. vinifera*), (Pierozzi and Moura, 2014) (Variety number *V*IVC 8540) grafted on IAC-572 rootstock were used for the experiments. Planted in 2006 in a commercial vineyard, berries were collected from two croppings: Oct 2021 to Jan 2022 and Oct 2022 to Dec 2022. From now on, they will be addressed as 2021 and 2022, respectively. The vineyard located in the municipality of São Fidélis, RJ, Brazil (21°51' S; 41°71' W), is constituted by plants in production distributed at 2.5 m between rows and 2 m between plants following in a pergola training system, and drip-irrigated by two emitters per plant at a distance of 0.5 cm from the stem. Berries were sampled during three developmental stages, following the Modified E-L system (Coombe, 1995): E-L 33, berries still hard and green; E-L 35, berries begin to colour and enlarge; and E-L 39, berries over-ripe. Five bunches per stage were collected by cutting the rachis and cold transported in transparent plastic bags inside a styrofoam box to the laboratory, located 1:30 h away by car.

3.2 Qualitative Trait Analysis

Five berries from each bunch were randomly selected to perform all of the analysis. The equatorial diameter was taken with a handheld electronic digital calliper (Digimess, Brazil). Berry firmness was carried out with a texture analyser (TA-XT, Stable Micro Systems, United Kingdom) equipped with a stainless steel plate, maintaining an intact pedicel. The measurement settings were a pre-test speed of 10 mm sec^{-1}, a test speed of 2 mm sec^{-1} and a post-test speed of 10 mm sec^{-1}, according to Lijavetzky et al. (2012). Firmness was measured and expressed as the force needed (Newton, N) to deform the berry by 20%. Berry juice was collected individually to evaluate total soluble solids (TSS, ºBrix) using an optical handheld refractometer with temperature compensation (model RHB-32/ ATC, Yhequipment, China). For titratable acidity (TA), the berries were peeled by inserting a stainless steel lab spoon/spatula between the pulp and skin; seeds were removed, and the pulp juice was collected by manual crushing in a mortar and pestle. The juice was then filtered in four layers of cheesecloth, diluted 10-fold with distilled water and three drops of 1% phenolphthalein were added to the samples, followed by titration with 0.1 N NaOH solution under stirring, until reaching pH 8.2. The results were expressed in gram of tartaric acid per 100 mL, calculated by the following equation (1):

$$ TA \ (g \ / \ 100 \ mL) = \frac{n \times N \times Eq}{10 \times V} \qquad \textbf{(1)} $$

Which:
n: volume of NaOH used in the titration;
N: NaOH normality (0.1 eq L^{-1});
Eq: equivalent weight of tartaric acid (75.04 g per eq);
V: berry juice volume (mL).

3.3 Mitochondria Isolation

Berries from 2021 were extracted according to Romieu and Flanzy (1988) with modifications. All procedures were held on ice and at 4ºC during centrifugations (Himac CP100NX, Hitachi Koki Life-Science, Japan). Distilled water was used in the preparation of all the buffers:

Extraction Buffer (EB): 0.3 mol L^{-1} Sucrose, 0.35 mol L^{-1} Mannitol, 1% (w/v) PVP-40, 5 mmol L^{-1} EDTA, 40 mmol L^{-1}, MOPS (pH 8), 0.1% (w/v) BSA;

Washing Buffer A (WBA): 0.3 mol L^{-1} Sucrose, 0.5 mol L^{-1} Mannitol, 1% (w/v) PVP-40, 1 mmol L^{-1} EDTA, 15 mmol L^{-1} Phosphate Buffer (pH 6.8), 0.5% (w/v) BSA;

Washing Buffer B (WBB): 0.3 mol L^{-1} Sucrose, 0.5 mol L^{-1} Mannitol, 0.5% (w/v) PVP-40, 1 mmol L^{-1} EDTA, 15 mM L^{-1} Phosphate Buffer (pH 7), 0.1% (w/v) BSA;

Resuspension Buffer (RB) - 0.3 mol L^{-1} Sucrose, 0.5 mol L^{-1} Mannitol, 10 mmol L^{-1} KCl, 5 mmol L^{-1} MgCl$_2$, 10 mmol L^{-1} Phosphate Buffer (pH 7.2), 0.1% (w/v) BSA.

Berries were peeled and seeds removed as described in 3.2. A 100 g portion of mesocarp was homogenized using a household blender/mixer (Oster, United States of America) three times for 3 s on low speed in 300 mL of EB (1:3 w/v). The pH was adjusted to 7.8 - 8.0 with 5 M NaOH. The resulting homogenate was filtered through four layers of cheesecloth and centrifuged for 40 min at 10,000 g. The supernatant was discarded and the pellet was resuspended with a soft bristle paint brush in 80 mL WBA, and then centrifuged for 15 min at 1,500 g. The supernatant was collected and centrifuged for 25 min at 10,000 g. The supernatant was discarded again and the pellet resuspended with 80 mL WBB, and then centrifuged for 20 min at 10,000 g. The supernatant obtained was discarded and the pellet, the crude mitochondrial fraction (CMF), was resuspended in 2.5-5 mL of MB.

For berries from 2022, glassware was cleaned with EtOH 70%. Centrifuge bottles (code 3127-0250 and 3139-0050, Nalgene, United States of America) were cleaned with hot boiling water followed by EtOH 70%. The cleaning method was applied to maintain detergent-free all the glass- and plasticware. The procedures were held in ice and 4 during centrifugations (Mega 21R, Hanil, South Korea). In the 2022 samples, the centrifugal order, time and speed were changed. For this, Verleur (1965), Bonner (1967), Douce et al. (1972), Millar et al. (2007), and Sweetlove et al. (2007), were consulted. To countermeasure different levels of acidity in each developmental stage, the concentration and pH of Tris-HCl on EB were modified accordingly. The pH was adjusted with 5 M NaOH or 21% Phosphoric Acid solution. Ultrapure water was used on the new buffers:

Extraction Buffer for E-L 33: 0.3 mol L^{-1} Sucrose, 0.35 mol L^{-1} Mannitol, 1% (w/v) PVP-40, 5 mmol L^{-1} EDTA, 400 mmol L^{-1} Tris-HCl (pH 8), 1% (w/v) BSA, 20 mmol L^{-1} Sodium Ascorbate (added just prior to extraction);

Extraction Buffer for E-L 35: 0.3 mol L^{-1} Sucrose, 0.35 mol L^{-1} Mannitol, 1% (w/v) PVP-40, 5 mmol L^{-1} EDTA, 300 mmol L^{-1} Tris-HCl (pH 7.4), 1% (w/v) BSA, 20 mmol L^{-1} Sodium Ascorbate;

Extraction Buffer for E-L 39: 0.3 mol L^{-1} Sucrose, 0.35 mol L^{-1} Mannitol, 1% (w/v) PVP-40, 5 mmol L^{-1} EDTA, 150 mmol L^{-1} Tris-HCl (pH 7.8), 1% (w/v) BSA, 20 mmol L^{-1} Sodium Ascorbate;

Washing Buffer (WB): 0.3 mol L^{-1} Sucrose, 0.35 mol L^{-1} Mannitol, 0.5% (w/v) PVP-40, 1 mmol L^{-1} EDTA, 15 mmol L^{-1} Phosphate Buffer (pH 7.2), 0.1% (w/v) BSA;

Resuspension Buffer (RB) was the same as above.

The berries were peeled and kept under EB in a proportion of 1:3 (w/v). Mesocarp and seeds were homogenized by manually crushing with a potato masher in circular movements inside a beaker. The resulting homogenate was filtered through six layers of cheesecloth and centrifuged for 15 min at 1,500 *g*. The supernatant was then centrifuged for 25 min at 10,000 *g* and the pellet was set loose using a soft bristle paintbrush in a small amount of WB. The solution was transferred to a Potter-Elvehjem PTFE pestle and glass tube of 8 mL and homogenized. The homogenate was then diluted in WB, centrifuged for 15 min at 2,000 *g* and the resulting supernatant was centrifuged for 20 min at 10,000 *g*. The pellet (CMF) was resuspended in 2-2.5 mL of MB with a soft artist paintbrush.

3.4 Mitochondrial Integrity Estimation

3.4.1 Fluorescence Microscopy of the Crude Mitochondrial Fraction

Mitochondria integrity from 2021 samples were accessed according to Vishwakarma and Gupta (2017). MitoTracker™ Red FM dye (500 nM L^{-1}) was added to 50 µL of freshly isolated mitochondria. To demonstrate that fluorescence signals emerged from mitochondria, we caused an osmotic shock to another set of samples by diluting 10-fold distilled water before adding the dye. Samples were

kept in the dark for 10 minutes at room temperature (RT). Afterwards, 3 µL of both suspensions were analysed by fluorescence microscopy (Zeiss Axio Imager A.2 HB 100, mounted with Axiocam MRc5 and AxioVision software, Germany) at RT, with an appropriate excitation (581 nm) and emission (644 nm) wavelength. Images were processed in Fiji software (Schindelin et al., 2012).

3.4.2 Outer Mitochondrial Membrane (OMM) Integrity

33-55 µg mL^{-1} of protein from the CMF was added to the assay mixture containing 0.1 M Tris-HCl buffer (pH 7.2). To start the reaction, 30 µmol L^{-1} of cytochrome C (final concentration) was added. By comparing the activity of Cytochrome-c Oxidase (Complex IV, COX, EC [Enzyme Commission Number] 7.1.1.9) before (slope a) and after the addition of non-ionic detergent (slope b), the integrity of the outer mitochondrial membrane (OMM) was estimated. 0,02% (v/v) of Triton X-100 (final concentration) was added to determine slope b. Equation 2 was used to calculate OMM Integrity:

$$OMM\ Integrity\ (\%) = \left(1 - \left(\frac{slope(a)}{slope(b)}\right)\right) \times 100 \qquad \textbf{(2)}$$

3.5 Quantification of Chlorophyll

An aliquot of 20 µl of crude mitochondrial fraction was diluted 50-fold in a mixture of acetone:distilled water (8:2) in a 1 cm quartz cuvette (Sigma-Aldrich Corporation, United States of America). The solution was measured spectrophotometrically, according to Arnon (1949) (Varian Cary 50 UV-Vis, Agilent Technologies, United States of America) at 645 nm and 663 nm and its absorbance was recorded. The results were interpreted with the Cary WinUV software (Agilent Technologies, United States of America) in the Advanced Reads application. A user collect result was performed following equation 3:

$$(20.2 \times ABS_{645} + 8.02 \times ABS_{663}) \times 0.05 \qquad \textbf{(3)}$$

3.6 Quantitation of Total Proteins

The protein estimation was held according to Bradford (1976) using Pierce™ Coomassie (Bradford) Protein Assay Kit (Thermo Fisher Scientific, United States of America). All measurements were performed in a 96-well microplate (Cralplast, Brazil). Following the Standard Microplate Protocol, 250 μl of Bradford Reagent were added in 5 μl of the sample, Bovine Serum Albumin standard curve and water blank. Absorbance measurements were taken at 595 nm with a microplate reader (μ-Quant, Bio-Tek Instruments, UK). KCJunior software (Bio-Tek Instruments, UK) was used to calculate the results.

3.7 Enzyme Activity of Crude Mitochondrial Fraction

The activity assays were measured spectrophotometrically (Varian Cary 50 UV-Vis, Agilent Technologies, United States of America) in a continuous assay for 1 to 2 min (0.1 to 0.5 s readings) in a 1.4 mL quartz cuvette (pathlength 10 mm, Sigma-Aldrich Corporation, United States of America). An Enzyme Assay Mixture without sample and substrate(s) was made fresh before every experiment. All components were stored during experiments in Thermo Shaker with cooling (model K80-120R, Kasvi, Brazil) set to 4 ºC. A concentration of 33-55 μg mL^{-1} from the CMF proteins was mixed by inversion before each measurement covering the top of the cuvette with Parafilm. Substrates were mixed either by inversion or by repeated pipetting/ejecting. The initial linear rate was calculated with a Zero Order Rate (equation 4), using the Cary WinUV software (Agilent Technologies, United States of America). Enzyme and substrate blanks were performed, and the absorbance difference between the sample and substrate was calculated. The enzymatic rate was calculated according to equation 5 (Punekar, 2018a), and the activity was expressed as the change in mmol or μmol μg protein^{-1} min^{-1} following equation 6 (Punekar, 2018b):

$$ABS = kt + ABS0 \qquad (4)$$

Which:
ABS: absorbance at time t
ABS0: absorbance at time t = 0
k: rate constant

t: time

$$\left(\frac{\Delta A}{t}\right)_{\text{enzymatic}} = \left(\frac{\Delta A}{t}\right)_{\text{Test}} - \left(\frac{\Delta A}{t}\right)_{\text{-S}} - \left(\frac{\Delta A}{t}\right)_{\text{-E}} \qquad \textbf{(5)}$$

Which:

ΔA/t = rate of absorbance change. -S, substrate blank; -E, enzyme blank

$$v = \frac{-\Delta A}{\varepsilon l} \times \frac{1}{\Delta t} \qquad \textbf{(6)}$$

Which:

ΔA: change of absorbance over time. From equation 4, abs/min. Therefore:

Δt: time variation: 1 min

ε: Molar absorption coefficient

l: cuvette pathlength

For berries from 2022, the activity was measured before and after freezing the samples. The berries from 2021 consisted only of frozen samples.

The cuvette was mounted on a rectangular water thermostatted cell holder (Agilent Technologies, United States of America), with circulating water in a constant flow of 360 L h^{-1} (XTPUMP - XT-360 5W, OceanTech, China) with temperature manually adjusted to 30 ± 1°C. The pump was attached to the side of a thermostatic bath (SBS, Europe) in which distilled water temperature was measured with a thermometer (Internal scale, Cod. 5003, Incoterm, Brazil).

3.7.1 Malate Dehydrogenase (MDH) (EC 1.1.1.37) Activity

According to Neuburger (1980) with modifications, MDH activity was measured in resuspension buffer (*see* **3.3 Mitochondria Isolation**), with the addition of 5 µg mL^{-1} antimycin A and 1 mmol L^{-1} oxaloacetate. The addition of 0.15 mmol L^{-1} NADH.H$^+$ started the reaction. The oxidation of NADH.H$^+$ to NAD$^+$ was registered at 340 nm (ε = 6220 M^{-1}) and the activity expressed as micromol of NADH oxidized per minute (µmol min^{-1}).

3.7.2 Succinate Dehydrogenase - Complex II (SDH) (EC 1.3.5.1) Activity

Soluble SDH activity was determined with 2,6-dichlorophenolindophenol (DCPIP) acting as an artificial electron acceptor. According to Romieu and Flanzy (1988) with modifications. The sample was added to the assay mixture containing 50 mmol L^{-1} phosphate buffer, 0.5 mmol L^{-1} EDTA (pH 7.8), 1 mmol L^{-1} KCN and 20 mmol L^{-1} succinate. The addition of 1 mmol L^{-1} PMS and 0.1 mmol L^{-1} DCPIP started the reaction. The reduction of DCPIP was registered at 600nm (ε = 19.1 mM^{-1}) and their activity expressed as micromol of DCPIP reduced per minute (μmol min^{-1}).

3.7.3 Fumarase (FH) (EC 4.2.1.2) Activity

According to Romieu and Flanzy (1988) with modifications, FH activity was measured in an assay mixture containing 50 mmol L^{-1} phosphate buffer, and 1 mmol L^{-1} EDTA (pH 7.2). The reaction was started with the addition of 20 mmol L^{-1} Malate. Fumarate appearance was followed directly at 240 nm (ε = 2.44 mM^{-1}) and their activity expressed as milimol of fumarate appeared per minute (mmol min^{-1}).

3.8 *In situ* fixation of Berry Mesocarp for Transmission Electron Microscopy

Berries from the 2022 sample were fixated according to Diakou and Carde, (2001) and Pérez-Bermúdez et al. (2017) with modifications. Disposable 1 mL syringes with 0.45 mm diameter needles were used to inject fixative (25% unbuffered glutaraldehyde) into the outer tissues and inner tissues of the whole berries. The fixative was injected slowly by hand until flowing up at the berry surface. Up to 20 injections in the exocarp and mesocarp were performed in each berry. After 24 h at RT, the proximal and distal sides of the berry closer to the seeds were cut into slices 2-2.5 mm thick and put in a fixative solution of 2.5% glutaraldehyde in 100 mM sodium phosphate buffer pH 7.2. For Green berries, equatorial slices 2-2.5 mm thick were cut without prior fixation and added to the fixative solution. All the samples were then rinsed with sodium phosphate buffer and incubated with buffered 1% osmium tetroxide for 1 h at RT. The specimens were then dehydrated through a series of acetone washes and embedded in Epon

resin. Ultrathin sections (80-90 nm thick) were collected on uncoated 400-mesh copper grids. After staining with 5% uranyl acetate for 30 min and then with 1% aqueous lead citrate for 5 minutes, the sections were observed with a JEM-1400 series 120kV Transmission Electron Microscope (JEOL, United States of America) operating at 80kV. Pictures were taken at direct magnifications from x800 to x2500. Brightness, contrast and smoothness of the images were processed in Fiji software (Schindelin et al., 2012). Raw .dm4 images were used to calculate Mitochondrial Cristae Density (MCD) and thickness from the tonoplast, cellular membrane, intercellular cell wall, the space between cell-cell wall and the starch granules area.

3.9 Statistical Analysis

Analysis and graphing were performed in "OriginPro 2021" software (v 9.8.0.200). Two-Way ANOVA (Factor A: Stage; Factor B, Year or CMF state) with interaction (Diametre; Total Soluble Solids; Total Protein; FH, MDH and SDH from 2022 samples; FH from frozen CMF samples) and One-Way ANOVA (Titrable Acitidy; Fresh Mass; Deformability; Total Chlorophyll; Integrated Density; OMM Integrity; MDH activity from frozen CMF samples) were performed, followed by *post-hoc* Tukey test for means comparison with significance level of 0.05. Two-sample t-test with significance level of 0.05 was performed to analyse measurements obtained from transmission electron microscopy (Group: Stage; Data: Measurement values), to compare MDH activity from frozen CMF samples and Total Chlorophyll values between stages from different years. All measurements shown are means ± SD.

4. RESULTS

4.1 Qualitative Traits

Berries sampled in 2021 had higher diametre when compared to berries sampled in 2022 (Fig. 2A). This may have lead to a lower TSS values (Fig. 2B). Titrable acidity was similar in both years (Fig. 2B). Despite the same diameter at E-L 33 and 39, 2021 berries were higher in TSS than in 2022. Deformability in 2022 berries decreased along development, while their fresh mass, increased (Figs. 2C and 2D).

4.2 Chlorophyll Concentration and Total Proteins

Both years' extraction followed a similar decrease of total chlorophyll, as expected by the natural depletion of chloroplasts in fruits, although 2022 values were higher at all stages (Fig. 3A).

Because different mesocarp fresh mass was used to extract mitochondria in 2022 stages (E-L 33, 100 g; E-L 35, 180 g; E-L 39, 163 g) and double volume of resuspension buffer was used on E-L 39 in 2021, the values were transformed to account it. When the same mesocarp fresh mass was used for extraction at all

stages in 2021 (100 g), the E-L 39 total protein concentration was higher (Fig. 3B). The same occurred in the 2022 samples. Moreover, the amount of protein extract in 2022 was higher than in 2021 samples in all stages.
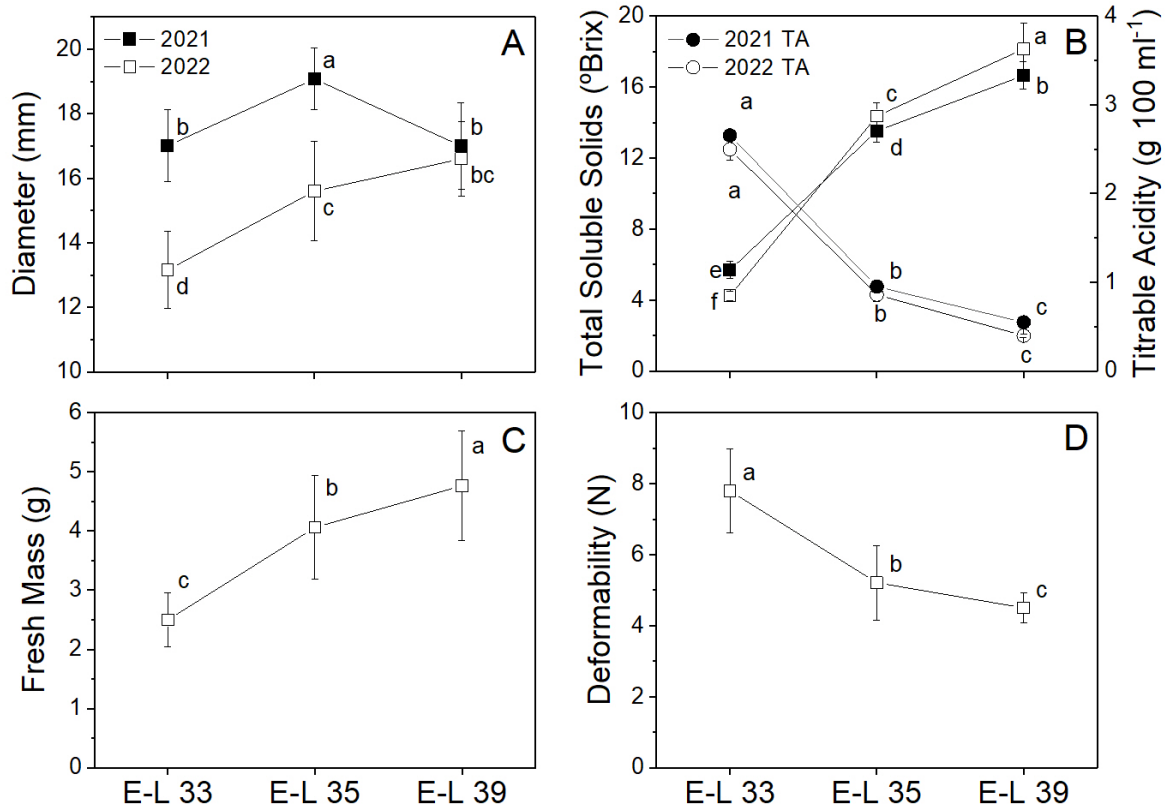
Figure 2. Berry qualitative trait from the stages sampled. E-L 33, berries still hard and green; E-L 35, berries begin to colour and enlarge; and E-L 39, berries over-ripe. Means that do not share a letter are significantly different. All values shown are means ± SD
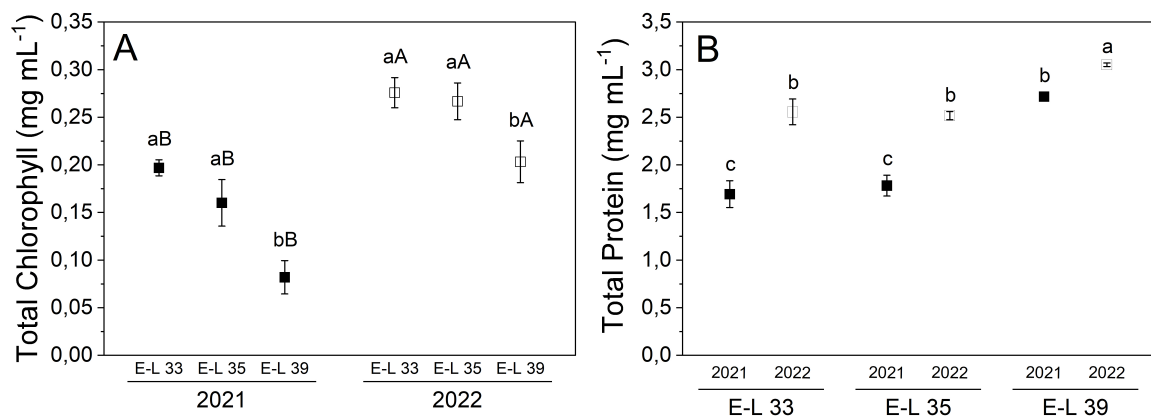
Figure 3. Total chlorophyll (A) and proteins (B) from the crude mitochondrial fraction in the different years and stages. In (A), low key letter represents the difference within stages from the same year and capital letters are the difference between the same stages. E-L 33, berries still hard and green; E-L 35, berries begin to colour and enlarge; and E-L 39, berries over-ripe. Means that do not share a letter are significantly different. All values shown are means ± SD

4.3 Mitochondrial Integrity

In 2021 berries we observed that fluorescence has increased at E-L 39 (Fig. 4A). Osmotic shock treatment decreased fluorescence to the same values as of pre-*veraison*. In mitochondria extracted in 2022, the outer mitochondrial membrane was intact at the *veraison* and post-*veraison* stages, but E-L 33 still maintained lower integrity (Fig. 4B).

4.4 Enzyme Activity of Crude Mitochondrial Fraction

Fumarase (FH) activities were detectable in all stages from both years. E-L 35 was the only stage that presented different activity values (Fig. 5A). Malate Dehydrogenase (MDH) E-L 33 activity was similar between years while later stages values were higher for 2022 when compared to 2021 (Fig. 5B). E-L 35 and 39 in 2021 samples were similarly lower while the decrease in 2022 was gradual. Succinate dehydrogenase (SDH) activity was not detectable in 2021 samples. Fresh E-L 33 SDH activity decreased when compared to the frozen CMF, being the opposite for E-L 39, where the frozen samples had higher activity. The same occurred for MDH at E-L 33 and 35, and FH at E-L 35 (Figs. 6A, 6B, and 6C).

4.5 Mesocarp Ultrastructure

Outer mesocarp at E-L 33 presented chloroplasts (Ch) with starch (S) and several mitochondria (M) (Figs. 7a and 7b). We identified the endoplasmatic reticulum (ER) and Golgi apparatus (GA) (Fig. 7b). Polyphenols (PP) were detected in the vacuole (V) (Fig. 7c). The visible cytoplasm was constricted in a thin layer. Intact tonoplast (arrow) and cell membranes (arrowhead) were observed in all samples. Intercellular cell walls (ICW) were electron dense and in close contact with the cells. At E-L 39, ICW lost their electron density, and the space between the cells and ICW became larger (Figs. 8a, 8b, 8c, and 8d, Table 1). In some samples, the ICW was not visible in the ultra thin cut. The same occurred to cells bearing both sides of the ICW (Figs. 7a, 7b, 7c, 7d, 7e, and 7f). The middle lamella (ML) was discontinuous throughout ICW (Figs. 8a, 8b, and 8c). M were

lower in number and cristae density (Table 1). The cytoplasmatic content was less electron dense.
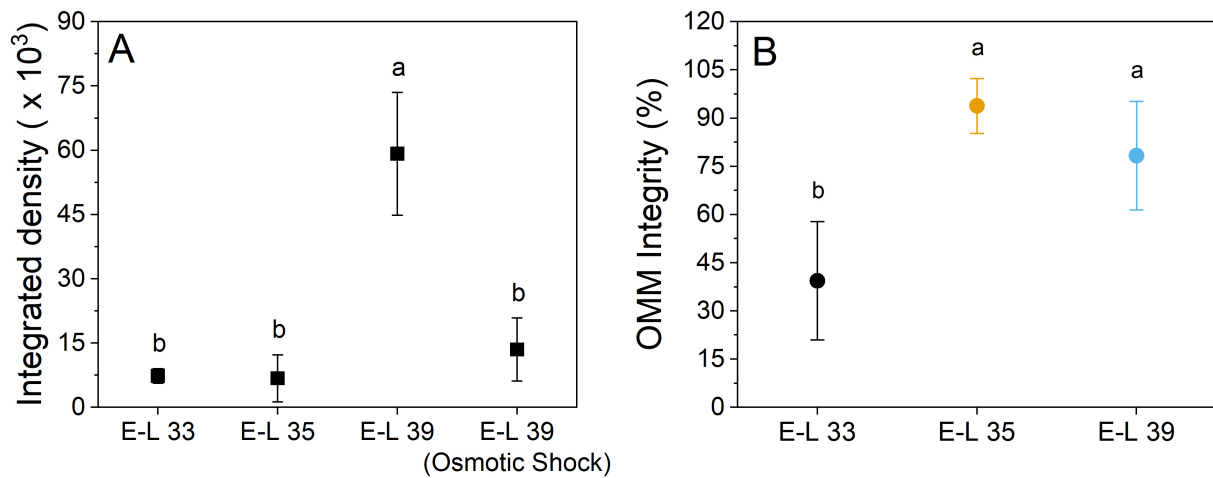
Figure 4. Membrane integrity from the crude mitochondrial fraction. Integrated density (A) of pixels from image fluorescence of samples from 2021 and Outer Membrane Integrity (OMM) (B) of samples from 2022. E-L 33, berries still hard and green; E-L 35, berries begin to colour and enlarge; and E-L 39, berries over-ripe. Means that do not share a letter are significantly different. All values shown are means ± SD
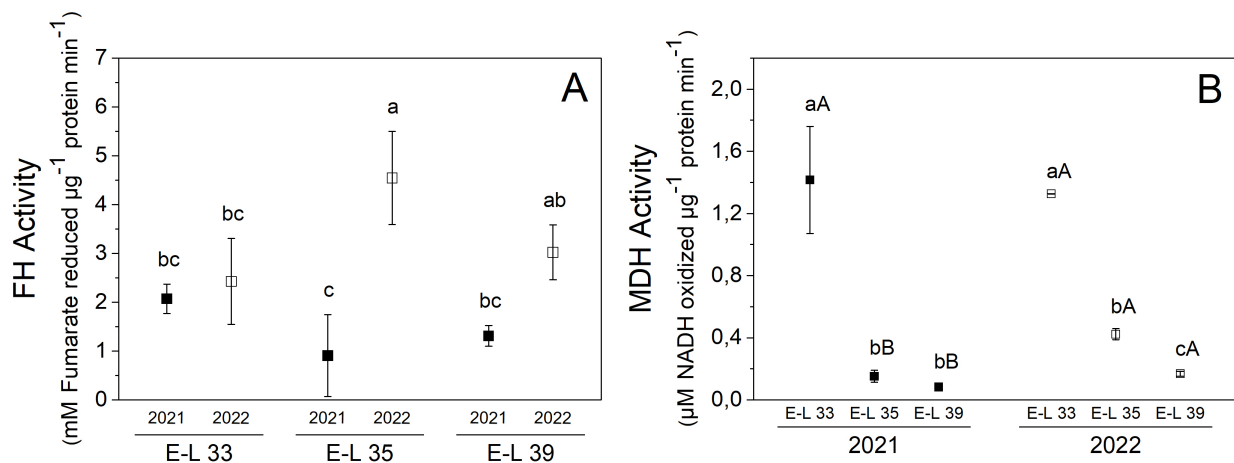
Figure 5. Enzymatic activity from fumarate (FH) (A) and malate dehydrogenase (MDH) (B) in frozen samples from the crude mitochondrial fraction. In (B), low key letter represents the difference within stages from the same year and capital letters are the difference between the same stages. E-L 33, berries still hard and green; E-L 35, berries begin to colour and enlarge; and E-L 39, berries over-ripe. Means that do not share a letter are significantly different. All values shown are means ± SD
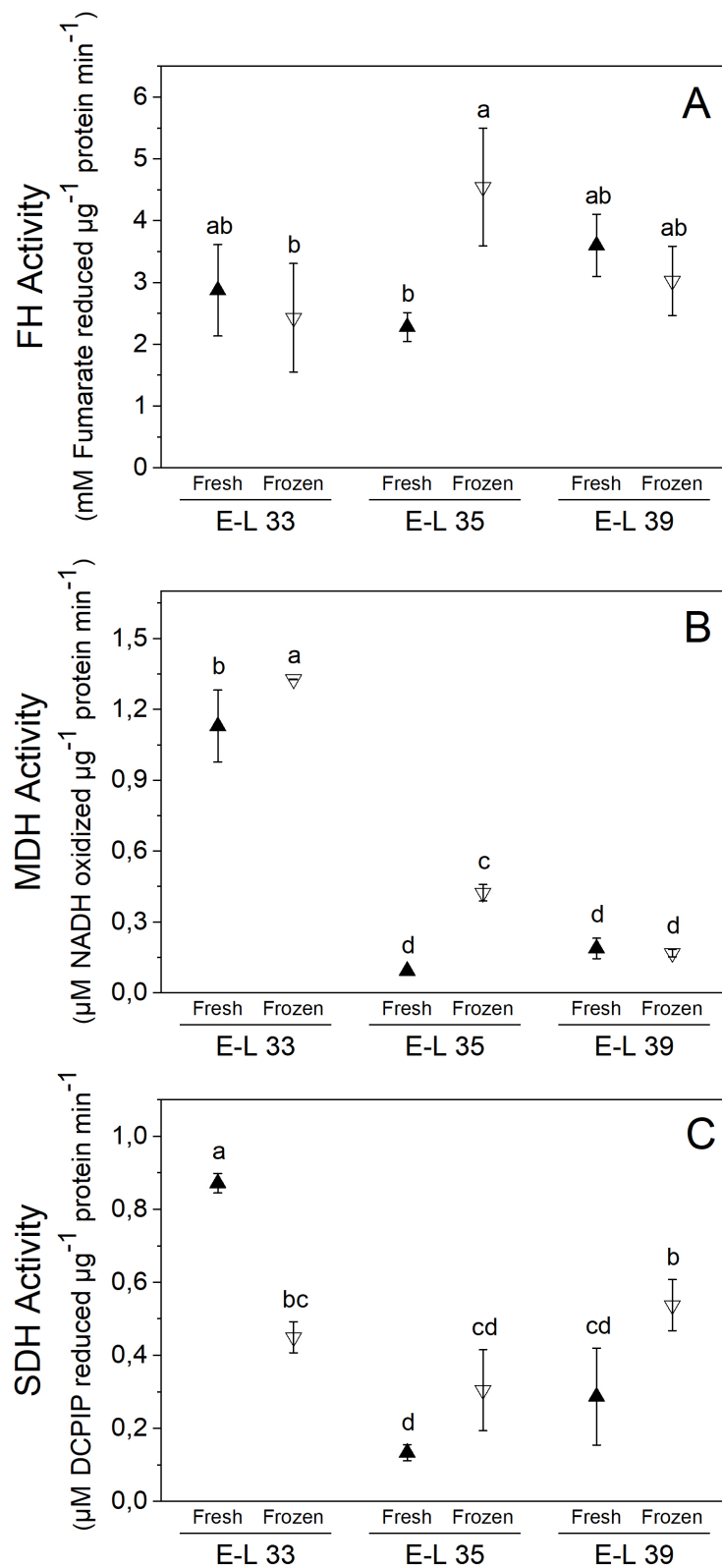
Figure 6. Enzymatic activity from fumarate (FH) (A), malate dehydrogenase (MDH) (B) and succinate dehydrogenase (SDH) (C) in fresh and frozen crude mitochondrial fraction samples. E-L 33, berries still hard and green; E-L 35, berries begin to colour and enlarge; and E-L 39, berries over-ripe. Means that do not share a letter are significantly different. All values shown are means ± SD
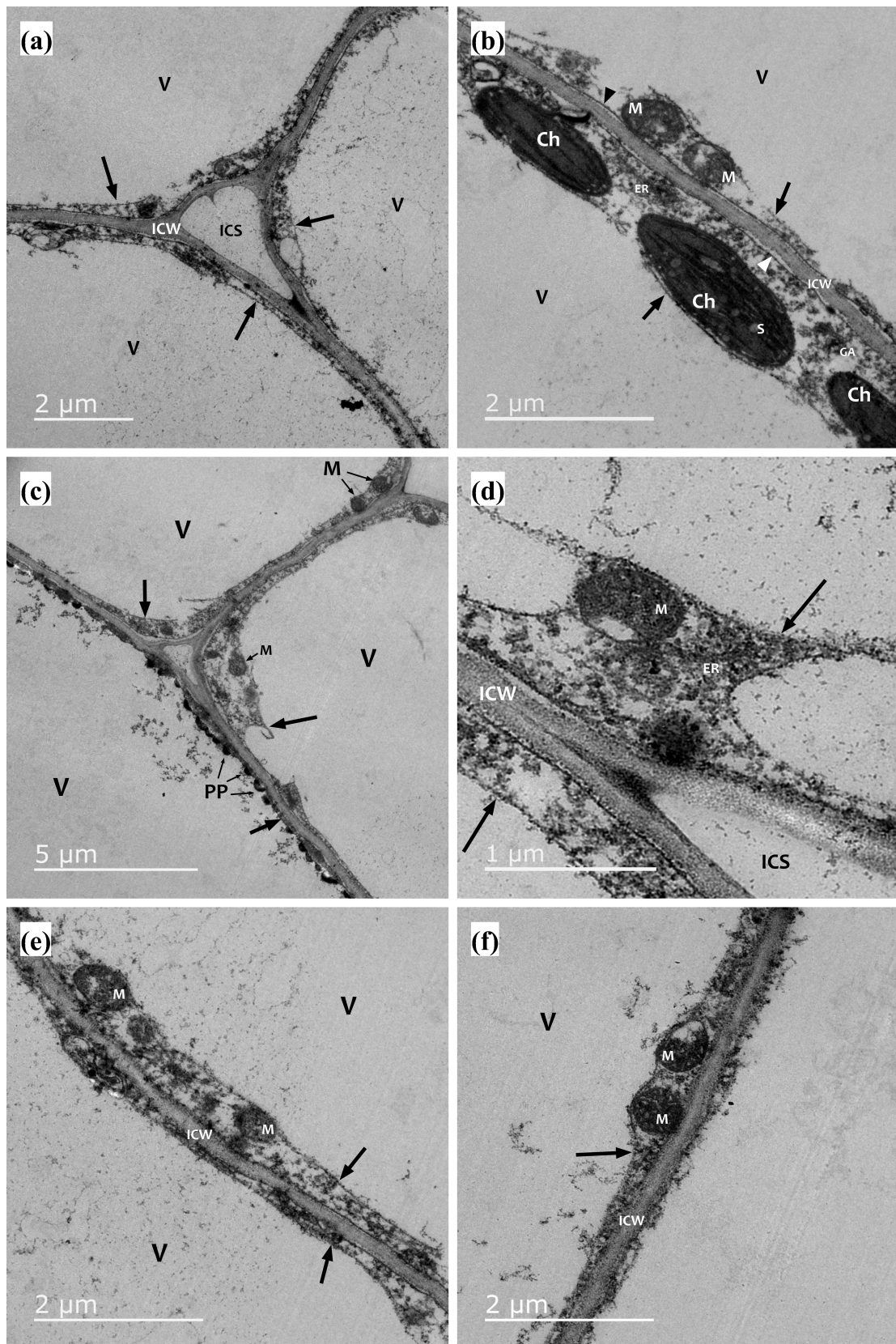
Figure 7. Ultrastructure from the mesocarp cells of *cv*. 'Niagara Rosada' at stage E-L 33, berries still hard and green. Arrow; tonoplast; Arrowhead, plasmatic membrane; Ch, chloroplast; ER, endoplasmatic reticulum; GA, golgi apparatus; ICS, intercellular space; ICW, intercellular wall; M, mitochondrion; ML, Middle lamella; PP, polyphenolics; S, starch; V, vacuole.
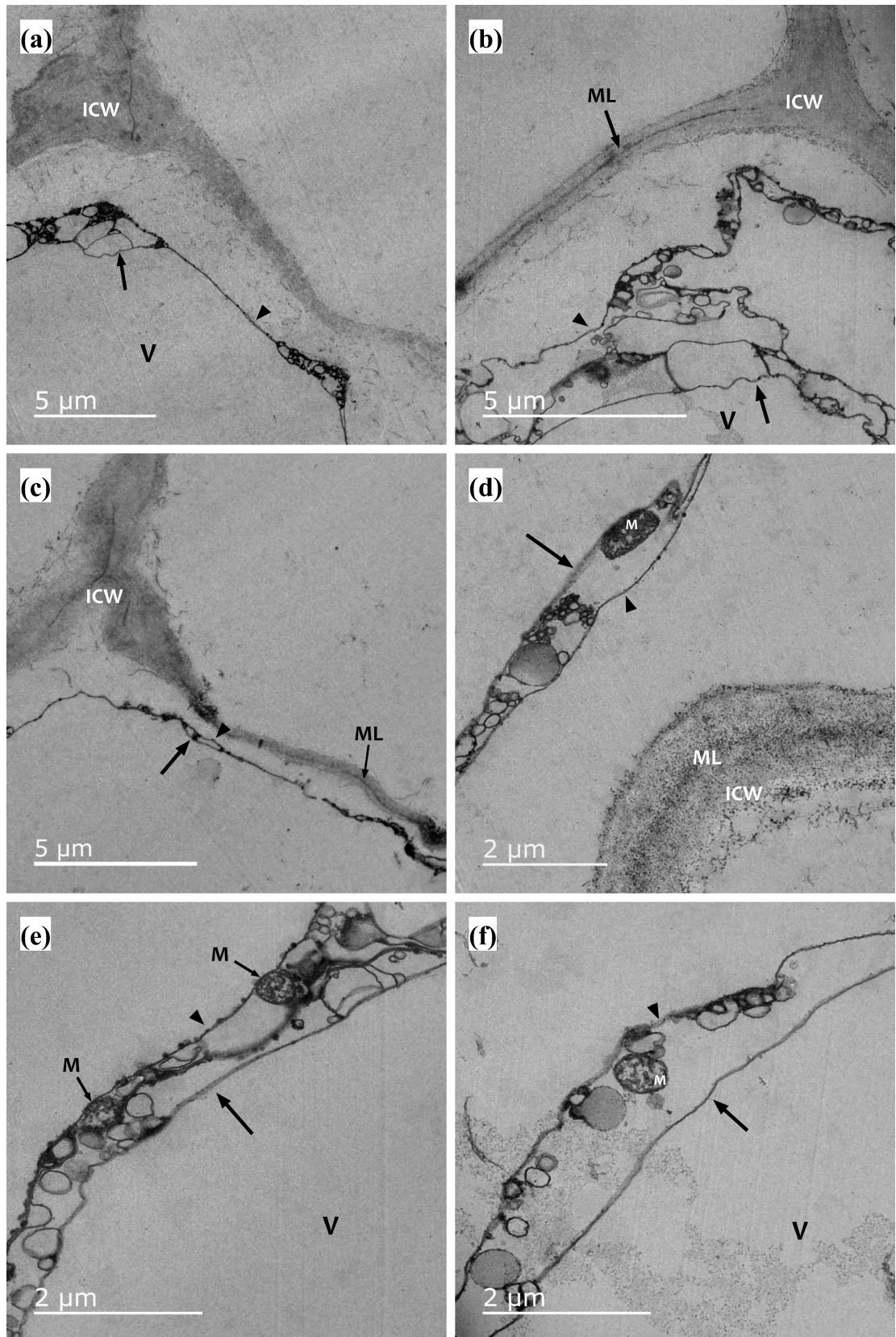
Figure 8. Ultrastructure from the mesocarp cells of *cv*. 'Niagara Rosada' at stage E-L 39, berries over-ripe. Arrow; tonoplast; Arrowhead, plasmatic membrane; ICW, intercellular wall; M, mitochondrion; ML, Middle lamella; PP, polyphenolics; S, starch; V, vacuole.

Table 1. Ultrastructure measurements from the mesocarp cells of cv. 'Niagara Rosada' at stage E-L 33, berries still hard and green and E-L 39, berries over-ripe. Means that do not share a letter are significantly different. ICW, intercellular wall; CM, plasmatic cell membrane; T, tonoplast; CM-CW, space between cell-cell wall; S, starch granule

Phenological stage	Thickness (µM)			Distance (µM)	Area (nm)	Mitochondrial Cristae Density (%)
	ICW	CM	T	CM-CW	S	
E-L 33	0.1785 ± 0.057 b	0.0146 ± 0.0046 b	0.017 ± 0.0057 b	0.0298 ± 0.019 b	6.3 ± 2.3	82.81 ± 10.54 a
E-L 39	0.8885 ± 0.388 a	0.0307 ± 0.0071 a	0.023 ± 0.0069 a	5.1231 ± 3.635 a	-	70.20 ± 3.93 b

5. DISCUSSION

We were able to isolate intact mitochondria at different stages in two consecutive years from the mesocarp of the *cv*. 'Niagara Rosada', is a cultivar that presents an early loss of mesocarp cell vitality. The combination of enzyme respiratory activity, mitochondria integrity and ultrastructure proved to be effective for testing the viability of berry mesocarp. The present data indicate that the loss of berry mesocarp integrity was not associated with cell death.

We detected lower fluorescence on the crude mitochondrial fraction (CMF) after the addition of MitoTracker Red in stages E-L 33 and 36 from 2021. The use of a household blender could be one source of mitochondria damage, leading to the extraction of non-intact mitochondria. However, E-L 39 berries exhibited higher fluorescence values, despite the use of a blender. Because MitoTracker Red fluorescence arises from mitochondrial membrane potential, membrane disruption by an osmotic shock would lessen fluorescence emission. By doing this, we demonstrated that the fluorescence originated indeed from intact mitochondria. Nonetheless, we changed the method of maceration to reduce the damage that could inherently originate from the blender, even on low velocities. The use of a potato smasher provided a gentle maceration of the mesocarp tissue, without excessive disorganization of mitochondria. Therefore, we needed another source

of damage to explain the integrity difference. The extraction buffer (EB) containing 40 mM MOPS did not hold high levels of acidity in early stages berries, leading to a final pH after maceration of around 3-3.5 for E-L 33 and 35, far from the 7.0-7.2 recommended (Millar et al., 2007). Change in EB resulted in improved isolation of intact mitochondria, as observed by outer mitochondrial membrane (OMM) integrity in 2022 berries, with similar values for later stages. 2022 E-L 33 berries were possibly damaged with maceration on a plastic tray (the berries were too hard and we were not able to macerate inside the beaker), where residues could have interfered with the extraction.

Further purification of the CMF was tried by sucrose gradient according to Douce et al. (1972) (data not shown). Because the yield is lower after purification, where only 5-15% of total mitochondria membrane marker enzyme activity in a tissue is found (Millar et al., 2007), the amount of starting tissue used in this work was possibly insufficient to yield enough viable mitochondria to perform this procedure. In addition, Romieu and Flanzy (1988) stated that if purification takes place in a sucrose gradient, the mitochondria separate into two contaminated peaks.

Møller et al. (2021) list some criteria for demonstrating successful isolation of functional and uncontaminated mitochondria, including the good coupling criteria. We extracted intact but not tightly-coupled mitochondria, as we were not able to get a polarographic response of oxygen consumption when testing for coupling efficiency in an Oxytherm+ system (Hansatech Instruments, United Kingdom) (data not shown), meaning that the addition of ADP did not stimulate oxygen uptake by extracted mitochondria.

The Inner mitochondrial membrane (IMM) is impermeable to NADH and organic acids. Therefore, by measuring soluble matrix enzymes activity before and after disruption of the membrane, we can estimate the integrity of the IMM. Consequently, MDH activity from 2022 stages E-L 33 and 35 can indicate IMM integrity. However, as stated by Rasmusson et al. (2021), MDH may follow mitochondria through the purification procedure (released from broken mitochondria or originated from the cytosol) leading to an underestimation of the IMM in some cases; this is supposed to happen to Fumarase (FH) at stages E-L 33 and 39. The other alternative would be malate being moved between the membranes via mitochondrial dicarboxylate/tricarboxylate transporters and being

readily available for FH. However, transporters' relative expression rises close to the onset of ripening, decreasing afterwards (Regalado et al., 2012). By applying Occam's Razor, the first one is more plausible.

Succinate dehydrogenase (SDH) activity was not observed in 2021 samples most probably because SDH formed aggregates after random solubilization in the medium during freezing-thawing, as shown by Hanstein et al. (1971) and Hederstedt and Rutberg (1981). Indeed, samples from 2021 revealed visible insoluble contents. Solubilization could have been prevented by the addition of Mg^{2+} (Neuburger, 1980; Pilchova et al., 2017) before freezing the material. In addition, the non-ionic detergent Triton X-100 could have been used to solubilize the aggregates. The lower activity in 2022 E-L 33 after freezing could be explained the same way.

Intact mitochondria with dense cristae observed by Transmission Electron Microscopy (TEM) images from berry mesocarp at E-L 33 indicate that FH and SDH activities before membrane disruption were most probably artefacts from the isolation. Cristae density decrease in E-L 39 correlates with a reduction of MDH and SDH activity, which are a marker enzyme or is embedded in the membrane. FH's high activity may be from the fact that the CMF had indeed a high concentration of mitochondria, despite their low abundance in the tissue later at ripening.

Malate degradation starts *ca* half a week after berry softening (Ruffner and Hawker, 1977), used in the detoxification of cytoplasm acidity caused by the exchange of H^+ for sucrose in the vacuoles (Shahood et al., 2020). Because malate degradation is mainly associated with mitochondrial MDH (mMDH) (Sweetman et al., 2009), its lower activity found at ripening in this work may suggest a different fate on malate degradation in 'Niagara Rosada'. One possibility is through its degradation in the gluconeogenesis pathway (Savoi et al., 2021). By proteomics, Garibaldi et al. (2007) and Martínez-Esteso et al. (2011) observed induced isoforms of glyceraldehyde-3-phosphate dehydrogenase (G3PDH) that may support gluconeogenesis after *veraison* in *cv*. Nebbiolo Lampia and *cv*. Muscat Hamburg, respectively. However, the first identified only lower cMDH quantity and the latter identified mMDH to be upregulated after *veraison*. In addition, transcriptomic data from *cv*. Syrah indicated the downregulation of several genes related to the glycolysis/gluconeogenesis pathways (Savoi et al.,

2021). Therefore, deeper work on proteomics (work in progress) and other enzyme activities are necessary to separate the varietal dependency that those pathways appear to present. An example is the MDH enzymatic activity of *cv*. Folle Blanche and *cv*. Thompson Seedless, the first was at a maximum at the ripen fruit stage (Belin Dal Peruffo and Pallavicini, 1975), contrarily to the latter where activity decreases during development (Hawker, 1969).

The mesocarp ultrastructure exhibited a generalized disorganization during ripening. Our results were similar to Da-peng et al. (1997) in *cv*. Kyoho (*V. vinifera x V. labrusca*), with cell cytoplasm almost electron-transparent, and "*a quantity of wadding debris of dissolved cytoplasmic components and some lipid bodies (...) left*". In our work, cell wall (CW) thickness was supposed to be higher as a response to expansin activity, an enzyme with the function of CW loosening. Indeed, in *cv*. Kyoho the expression of the expansin gene *VIexp2* is constantly higher after *veraison* (Ishimaru et al., 2007). Arabinogalactan proteins (AGPs) are another set of enzymes involved in the CW loosening process (Leszczuk et al., 2020), increasing from *veraison* in *cv*. Cabernet Sauvignon and *cv*. Crimson Seedless, with higher values at ripening (Moore et al., 2014). Furthermore, Nunan et al. (2001) identified hydrolases that modify CW fine structure. Therefore, despite higher thickness in E-L 39 stage, CW became less electron-dense, which might be caused by the hydrolysis or solubilization of CW polysaccharides. CW thickness from NR berries was 1.8-9-fold higher than reported for other cultivars (Diakou and Carde, 2001).

6. CONCLUSION

Our data indicate that the loss of berry mesocarp integrity was not associated with cell death. Cells from the outer mesocarp of 'Niagara Rosada' berry changes over ripening, exhibiting large spaces separating them, while the intercellular cell wall became less electron dense. The mitochondria remained intact but in lower numbers throughout development, even with mesocarp cell viability loss. Mitochondria extracted from the same tissue were uncoupled but intact, with outer and inner membranes viable. We determined enzymatically that malate dehydrogenase and succinate dehydrogenase enzymes presented lower activities in post-*veraison*, while fumarase remained constant. Those results proved to be effective for testing the viability of berry mesocarp.

BIBLIOGRAPHIC REFERENCES

Arnon, D. I. (1949). Copper enzymes in isolated chloroplasts. Polyphenoloxidase in *Beta vulgaris*. Plant physiology, 24(1), 1-15.

Bezerra L. B. S. (2018). Perda prematura de vitalidade celular em bagas de *Vitis labrusca* L. Dissertação (Mestrado em Produção Vegetal) - Campos dos Goytacazes – RJ, Universidade Estadual do Norte Fluminense – UENF, 58.

Bonada, M., Sadras, V., Moran, M., & Fuentes, S. (2013a). Elevated temperature and water stress accelerate mesocarp cell death and shrivelling, and decouple sensory traits in Shiraz berries. Irrigation Science, 31, 1317-1331.

Bonada, M., Sadras, V. O., & Fuentes, S. (2013b). Effect of elevated temperature on the onset and rate of mesocarp cell death in berries of Shiraz and Chardonnay and its relationship with berry shrivel. Australian Journal of Grape and Wine Research, 19(1), 87-94.

Bondada, B. R., Matthews, M. A., & Shackel, K. A. (2005). Functional xylem in the post-veraison grape berry. Journal of Experimental Botany, 56(421), 2949-2957.

Bonner Jr, W. D. (1967). [24] A general method for the preparation of plant mitochondria. In Estabrook R. W., Pullman M. E. (Vol. 10) Methods in Enzymology, 126-133.

Boss, P. K., & Davies, C. (2009). Molecular biology of anthocyanin accumulation in grape berries. In: Roubelakis-Angelakis, K. A. (org) Grapevine Molecular Physiology & Biotechnology (7 ed), 263-292.

Bradford, M. M. (1976). A rapid and sensitive method for the quantitation of microgram quantities of protein utilizing the principle of protein-dye binding. Analytical Biochemistry, 72(1-2), 248-254.

Caravia, L., Collins, C., & Tyerman, S. D. (2015). Electrical impedance of S hiraz berries correlates with decreasing cell vitality during ripening. Australian Journal of Grape and Wine Research, 21(3), 430-438.

Carlomagno, A., Novello, V., Ferrandino, A., Genre, A., Lovisolo, C., & Hunter, J. J. (2018). Pre-harvest berry shrinkage in cv 'Shiraz' (*Vitis vinifera* L.): Understanding sap flow by means of tracing. Scientia Horticulturae, 233, 394-406.

Castellarin, S. D., Bavaresco, L., Falginella, L., Gonçalves, M. I. V. Z., Di Gaspero, G., Gerós, H., ... & Delrot, S. (2012). Phenolics in grape berry and key antioxidants. The Biochemistry of the Grape Berry, 22, 89-110.

Chatelet, D. S., Rost, T. L., Shackel, K. A., & Matthews, M. A. (2008a). The peripheral xylem of grapevine (*Vitis vinifera*). 1. Structural integrity in post-veraison berries. Journal of Experimental Botany, 59(8), 1987-1996.

Chatelet, D. S., Rost, T. L., Matthews, M. A., & Shackel, K. A. (2008b). The peripheral xylem of grapevine (*Vitis vinifera*) berries. 2. Anatomy and development. Journal of Experimental Botany, 59(8), 1997-2007.

Choat, B., Gambetta, G. A., Shackel, K. A., & Matthews, M. A. (2009). Vascular function in grape berries across development and its relevance to apparent hydraulic isolation. Plant Physiology, 151(3), 1677-1687.

Clarke, S. J., & Rogiers, S. Y. (2019). The role of fruit exposure in the late season decline of grape berry mesocarp cell vitality. Plant Physiology and Biochemistry, 135, 69-76.

Coombe, B. G. (1976). The development of fleshy fruits. Annual Review of Plant Physiology, 27(1), 207-228.

Coombe, B. G. (1995). Growth stages of the grapevine: adoption of a system for identifying grapevine growth stages. Australian Journal of Grape and Wine Research, 1(2), 104-110.

Coombe, B. G., & Hale, C. R. (1973). The hormone content of ripening grape berries and the effects of growth substance treatments. Plant Physiology, 51(4), 629-634.

Dal Peruffo, A. B., & Pallavicini, C. (1975). Enzymatic changes associated with ripening of grape berries. Journal of the Science of Food and Agriculture, 26(5), 559-566.

Da-peng, Z., Min, L., & Yi, W. (1997). Ultrastructural changes in the mesocarp cells of grape berry during its development. Journal of Integrative Plant Biology, 54(4), 1121-1131.

Delrot, S., Picaud, S., & Gaudillere, J. P. (2001). Water transport and aquaporins in grapevine. In Roubelakis-Angelakis, K. A. (org) Molecular Biology & Biotechnology of the Grapevine (1 ed), 241-262.

Diakou, P., & Carde, J. P. (2001). In situ fixation of grape berries. Protoplasma, 218(3-4), 225-235.

Douce, R., Christensen, E. L., & Bonner Jr, W. D. (1972). Preparation of intact plant mitochondria. Biochimica et Biophysica Acta (BBA)-Bioenergetics, 275(2), 148-160.

Dreier, L. P., Hunter, J. J., & Ruffner, H. P. (1998). Invertase activity, grape berry development and cell compartmentation. Plant Physiology and Biochemistry, 36(12), 865-872.

Famiani, F., Farinelli, D., Palliotti, A., Moscatello, S., Battistelli, A., & Walker, R. P. (2014). Is stored malate the quantitatively most important substrate utilised by respiration and ethanolic fermentation in grape berry pericarp during ripening? Plant Physiology and Biochemistry, 76, 52-57.

Famiani, F., Farinelli, D., Frioni, T., Palliotti, A., Battistelli, A., Moscatello, S., & Walker, R. P. (2016). Malate as substrate for catabolism and gluconeogenesis during ripening in the pericarp of different grape cultivars. Biologia Plantarum, 60, 155-162.

Famiani, F., Walker, R. P., Tecsi, L., Chen, Z. H., Proietti, P., & Leegood, R. C. (2000). An immunohistochemical study of the compartmentation of metabolism during the development of grape (*Vitis vinifera* L.) berries. Journal of Experimental Botany, 51(345), 675-683.

Fontes, N., Côrte-Real, M., & Gerós, H. (2011). New observations on the integrity, structure, and physiology of flesh cells from fully ripened grape berry. American Journal of Enology and Viticulture, 62(3), 279-284.

Fuentes, S., Sullivan, W., Tilbrook, J., & Tyerman, S. (2010). A novel analysis of grapevine berry tissue demonstrates a variety-dependent correlation between tissue vitality and berry shrivel. Australian Journal of Grape and Wine Research, 16(2), 327-336.

Giribaldi, M., Perugini, I., Sauvage, F. X., & Schubert, A. (2007). Analysis of protein changes during grape berry ripening by 2-DE and MALDI-TOF. Proteomics, 7(17), 3154-3170.

Goulao, L. F., & Oliveira, C. M. (2008). Cell wall modifications during fruit ripening: when a fruit is not the fruit. Trends in Food Science & Technology, 19(1), 4-25.

Hanstein, W. G., Davis, K. A., Ghalambor, M. A., & Hatefi, Y. (1971). Succinate dehydrogenase. II. Enzymatic properties. Biochemistry, 10(13), 2517-2524.

Hawker, J. S. (1969). Changes in the activities of malic enzyme, malate dehydrogenase, phosphopyruvate carboxylase and pyruvate decarboxylase during the development of a non-climacteric fruit (the grape). Phytochemistry, 8(1), 19-23.

Hederstedt, L. A. R. S., & Rutberg, L. A. R. S. (1981). Succinate dehydrogenase--a comparative review. Microbiological Reviews, 45(4), 542-555.

Iland, P., Dry, P., Proffitt, T., & Tyerman, S. D. (2011). The grapevine: from the science to the practice of growing vines for wine. Adelaide, Patrick Iland Wine Promotions Pty Ltd, 320p.

Ishimaru, M., Smith, D. L., Gross, K. C., & Kobayashi, S. (2007). Expression of three expansin genes during development and maturation of Kyoho grape berries. Journal of Plant Physiology, 164(12), 1675-1682.

Jackson, R. S. (2008). Wine science: principles and applications. 3. ed. Academic Press, 776p.

Juan, K. A. N., Wang, H. M., & Jin, C. H. (2011). Changes of reactive oxygen species and related enzymes in mitochondrial respiration during storage of harvested peach fruits. Agricultural Sciences in China, 10(1), 149-158.

Keller, M., Smith, J. P., & Bondada, B. R. (2006). Ripening grape berries remain hydraulically connected to the shoot. Journal of Experimental Botany, 57(11), 2577-2587.

Keller, M., & Shrestha, P. M. (2014). Solute accumulation differs in the vacuoles and apoplast of ripening grape berries. Planta, 239, 633-642.

Keller, M., Zhang, Y. U. N., Shrestha, P. M., Biondi, M., & Bondada, B. R. (2015). Sugar demand of ripening grape berries leads to recycling of surplus phloem water via the xylem. Plant, Cell & Environment, 38(6), 1048-1059.

Keller, M. (2020). The Science of Grapevines. 3 ed. Cambridge, Academic Press, 554p.

Knipfer, T., Fei, J., Gambetta, G. A., McElrone, A. J., Shackel, K. A., & Matthews, M. A. (2015). Water transport properties of the grape pedicel during fruit development: insights into xylem anatomy and function using microtomography. Plant Physiology, 168(4), 1590-1602.

Krasnow, M., Matthews, M., & Shackel, K. (2008). Evidence for substantial maintenance of membrane integrity and cell viability in normally developing grape (*Vitis vinifera* L.) berries throughout development. Journal of Experimental Botany, 59(4), 849-859.

Lang, A., & Düring, H. (1991). Partitioning control by water potential gradient: evidence for compartmentation breakdown in grape berries. Journal of Experimental Botany, 42(9), 1117-1122.

Lerin J (2016). Propriedades hidráulicas em bagas em desenvolvimento de *Vitis labrusca* L. Cv. Niagara Rosada: relação entre vitalidade do mesocarpo e funcionalidade do xilema. Dissertação (Mestrado em Produção Vegetal) - Campos dos Goytacazes - RJ, Universidade Estadual do Norte Fluminense - UENF, 71.

Leszczuk, A., Kalaitzis, P., Blazakis, K. N., & Zdunek, A. (2020). The role of arabinogalactan proteins (AGPs) in fruit ripening—a review. Horticulture Research, 7(1):176.

Lijavetzky, D., Carbonell-Bejerano, P., Grimplet, J., Bravo, G., Flores, P., Fenoll, J., ... & Martinez-Zapater, J. M. (2012). Berry flesh and skin ripening features in *Vitis vinifera* as assessed by transcriptional profiling. PloS one, 7(6), e39547.

Martínez-Esteso, M. J., Sellés-Marchart, S., Lijavetzky, D., Pedreño, M. A., & Bru-Martínez, R. (2011). A DIGE-based quantitative proteomic analysis of grape berry flesh development and ripening reveals key events in sugar and organic acid metabolism. Journal of Experimental Botany, 62(8), 2521-2569.

Martínez-Esteso, M. J., Vilella-Antón, M. T., Pedreño, M. Á., Valero, M. L., & Bru-Martínez, R. (2013). iTRAQ-based protein profiling provides insights into the central metabolism changes driving grape berry development and ripening. BMC Plant Biology, 13, 1-20.

Matthews, M. A., & Shackel, K. A. (2005). Growth and water transport in fleshy fruit. In Holbrook N. M., Zwieniecki M. A. (eds.) Vascular transport in plants. Cambridge, Academic Press, pp. 181-197.

Matthews, M. A., Thomas, T. R., & Shackel, K. A. (2009). Fruit ripening in *Vitis vinifera* L.: possible relation of veraison to turgor and berry softening. Australian Journal of Grape and Wine Research, 15(3), 278-283.

May, P. (2000). From bud to berry, with special reference to inflorescence and bunch morphology in *Vitis vinifera* L. Australian Journal of Grape and Wine Research, 6(2), 82-98.

Millar, A. H., Liddell, A., & Leaver, C. J. (2007). Isolation and subfractionation of mitochondria from plants. Methods in Cell Biology, 80, 65-90.

Møller, I. M. (2001). Plant mitochondria and oxidative stress: electron transport, NADPH turnover, and metabolism of reactive oxygen species. Annual Review of Plant Biology, 52(1), 561-591.

Møller, I. M., Rasmusson, A. G., & Van Aken, O. (2021). Plant mitochondria–past, present and future. The Plant Journal, 108(4), 912-959.

Moore, J. P., Fangel, J. U., Willats, W. G., & Vivier, M. A. (2014). Pectic-β (1, 4)-galactan, extensin and arabinogalactan–protein epitopes differentiate ripening stages in wine and table grape cell walls. Annals of Botany, 114(6), 1279-1294.

Noctor, G., & Foyer, C. H. (2016). Intracellular redox compartmentation and ROS-related communication in regulation and signaling. Plant Physiology, 171(3), 1581-1592.

Noodén, L. D. (ed.) (2003). Plant cell death processes. Cambridge, Academic Press, 392p.

Nunan, K. J., Sims, I. M., Bacic, A., Robinson, S. P., & Fincher, G. B. (1998). Changes in cell wall composition during ripening of grape berries. Plant Physiology, 118(3), 783-792.

Nunan, K. J., Davies, C., Robinson, S. P., & Fincher, G. B. (2001). Expression patterns of cell wall-modifying enzymes during grape berry development. Planta, 214, 257-264.

Oberle, G.D. (1938) A genetic study of variations in floral morphology and functions incultivated forms of Vitis. New York State Agriculture Experimental Station.

Pérez-Bermúdez, P., Blesa, J., Soriano, J. M., & Marcilla, A. (2017). Extracellular vesicles in food: Experimental evidence of their secretion in grape fruits. European Journal of Pharmaceutical Sciences, 98, 40-50.

Pierozzi, N. I., & Moura, M. F. (2014). Cytological Analyses in 'Niagara Branca' Grape and in Its Somatic Mutant 'Niagara Rosada'. Notulae Botanicae Horti Agrobotanici Cluj-Napoca, 42(2), 460-465.

Pilati, S., Brazzale, D., Guella, G., Milli, A., Ruberti, C., Biasioli, F., ... & Moser, C. (2014). The onset of grapevine berry ripening is characterized by ROS

accumulation and lipoxygenase-mediated membrane peroxidation in the skin. BMC Plant Biology, 14(1), 1-15.

Pilchova, I., Klacanova, K., Tatarkova, Z., Kaplan, P., & Racay, P. (2017). The involvement of Mg2+ in regulation of cellular and mitochondrial functions. Oxidative medicine and cellular longevity, 2017:6797460.

Pires E. J. (1998) Emprego de reguladores de crescimento em viticultura tropical. Informe Agropecuário, 19(194), 40-57.

Pratt, C. (1971). Reproductive anatomy in cultivated grapes-a review. American Journal of Enology and Viticulture, 22(2), 92-109.

Punekar, N. S. (2018a). Good Kinetic Practices. In Punekar, N. S. ENZYMES: Catalysis, Kinetics and Mechanisms. 1 ed. 131-142.

Punekar, N. S. (2018b). Principles of enzyme assays. In Punekar, N. S. ENZYMES: Catalysis, Kinetics and Mechanisms. 1. ed pp.115-129.

Qin, G., Meng, X., Wang, Q., & Tian, S. (2009). Oxidative damage of mitochondrial proteins contributes to fruit senescence: a redox proteomics analysis. Journal of Proteome Research, 8(5), 2449-2462.

Rasmusson, A. G., Hao, M., & Møller, I. M. (2022). Integrity Assessment of Isolated Plant Mitochondria. In Van Aken, V., Rasmusson A. G. (eds) Plant Mitochondria: Methods and Protocols 1 ed. 51-62.

Regalado, A., Pierri, C. L., Bitetto, M., Laera, V. L., Pimentel, C., Francisco, R., ... & Agrimi, G. (2013). Characterization of mitochondrial dicarboxylate/tricarboxylate transporters from grape berries. Planta, 237, 693-703.

Ribéreau-Gayon, P., Dubourdieu, D., Donèche, B., & Lonvaud, A. (eds.) (2006) Handbook of enology, Volume 1: The microbiology of wine and vinifications. 2 ed. Hoboken, John Wiley & Sons, 497p.

Riebel, M., Fronk, P., Distler, U., Tenzer, S., & Decker, H. (2017). Proteomic profiling of German Dornfelder grape berries using data-independent acquisition. Plant Physiology and Biochemistry, 118, 64-70.

Romieu, C., & Flanzy, C. (1988). Extraction des mitochondries de baies de raisin (*Vitis vinifera*). Plant Physiology and Biochemistry, 26(5), 589-596.

Romieu, C., Tesniere, C., Than-Ham, L., Flanzy, C., & Robin, J. P. (1992). An examination of the importance of anaerobiosis and ethanol in causing injury to grape mitochondria. American Journal of Enology and Viticulture, 43(2), 129-133.

Ruffner, H. P., & Hawker, J. S. (1977). Control of glycolysis in ripening berries of Vitis vinifera. Phytochemistry, 16(8), 1171-1175.

Saladié, M., Matas, A. J., Isaacson, T., Jenks, M. A., Goodwin, S. M., Niklas, K. J., ... & Rose, J. K. (2007). A reevaluation of the key factors that influence tomato fruit softening and integrity. Plant Physiology, 144(2), 1012-1028.

Sarry, J. E., Sommerer, N., Sauvage, F. X., Bergoin, A., Rossignol, M., Albagnac, G., & Romieu, C. (2004). Grape berry biochemistry revisited upon proteomic analysis of the mesocarp. Proteomics, 4(1), 201-215.

Savoi, S., Torregrosa, L., & Romieu, C. (2021). Transcripts switched off at the stop of phloem unloading highlight the energy efficiency of sugar import in the ripening *V. vinifera* fruit. Horticulture Research, 8:193.

Schindelin, J., Arganda-Carreras, I., Frise, E., Kaynig, V., Longair, M., Pietzsch, T., ... & Cardona, A. (2012). Fiji: an open-source platform for biological-image analysis. Nature Methods, 9(7), 676-682.

Sentelhas P. C. (1998) Aspectos climáticos para a viticultura tropical. Viticultura tropical. Informe Agropecuário, 19 (194):9-14.

Shackel, K. A., Greve, C., Labavitch, J. M., & Ahmadi, H. (1991). Cell turgor changes associated with ripening in tomato pericarp tissue. Plant Physiology, 97(2), 814-816.

Shahood, R., Torregrosa, L., Savoi, S., & Romieu, C. (2020). First quantitative assessment of growth, sugar accumulation and malate breakdown in a single ripening berry. Oeno One, 54(4), 1077-1092.

Sweetlove, L. J., Taylor, N. L., & Leaver, C. J. (2007). Isolation of intact, functional mitochondria from the model plant Arabidopsis thaliana. In Leister, D., Herrmann J. M. (eds) Mitochondria: Practical Protocols. 1 ed. pp.125-136.

Sweetman, C., Deluc, L. G., Cramer, G. R., Ford, C. M., & Soole, K. L. (2009). Regulation of malate metabolism in grape berry and other developing fruits. Phytochemistry, 70(11-12), 1329-1344.

Terrier, N., & Romieu, C. (2001). Grape berry acidity. In Roubelakis-Angelakis, K. A. (eds) Molecular Biology & Biotechnology of the Grapevine. 1 ed. pp.35-57.

Tesniere, C., Pradal, M., El-Kereamy, A., Torregrosa, L., Chatelet, P., Roustan, J. P., & Chervin, C. (2004). Involvement of ethylene signalling in a non-climacteric fruit: new elements regarding the regulation of ADH expression in grapevine. Journal of Experimental Botany, 55(406), 2235-2240.

Thomas, T. R., Matthews, M. A., & Shackel, K. A. (2006). Direct in situ measurement of cell turgor in grape (*Vitis vinifera* L.) berries during development and in response to plant water deficits. Plant, Cell & Environment, 29(5), 993-1001.

Thomas, T. R., Shackel, K. A., & Matthews, M. A. (2008). Mesocarp cell turgor in *Vitis vinifera* L. berries throughout development and its relation to firmness, growth, and the onset of ripening. Planta, 228, 1067-1076.

Thompson, J. E. (1988). The molecular basis for membrane deterioration during senescence. In Noodén L. D., Leopold A. C. (eds) Senescence and aging in plants. Cambridge, Academic Press. pp.51-83

Tian, S., Qin, G., & Li, B. (2013). Reactive oxygen species involved in regulating fruit senescence and fungal pathogenicity. Plant Molecular Biology, 82, 593-602.

Tilbrook, J., & Tyerman, S. (2006). Water, sugar and acid: how and where they come and go during berry ripening. In Oag D., De Garis K., Partridge S., Dundon C., Francis M., Johnstone R., Hamilton R. (eds) Australian Society of Viticulture and Oenology: finishing the job – optimal ripening of Cabernet Sauvignon and Shiraz, 4-12

Tilbrook, J., & Tyerman, S. D. (2008). Cell death in grape berries: varietal differences linked to xylem pressure and berry weight loss. Functional Plant Biology, 35(3), 173-184.

Tilbrook, J., & Tyerman, S. D. (2009). Hydraulic connection of grape berries to the vine: varietal differences in water conductance into and out of berries, and potential for backflow. Functional Plant Biology, 36(6), 541-550.

Tong, C., Krueger, D., Vickers, Z., Bedford, D., Luby, J., El-Shiekh, A., ... & Ahmadi, H. (1999). Comparison of softening-related changes during storage of 'Honeycrisp' apple, its parents, and 'Delicious'. Journal of the American Society for Horticultural Science, 124(4), 407-415.

Tyerman, S. D., Tilbrook, J., Pardo, C., Kotula, L., Sullivan, W., & Steudle, E. (2004). Direct measurement of hydraulic properties in developing berries of *Vitis vinifera* L. cv Shiraz and Chardonnay. Australian Journal of Grape and Wine Research, 10(3), 170-181.

Verleur, J. D. (1965). Studies on the isolation of mitochondria from potato tuber tissue. Plant Physiology, 40(6), 1003.

Vishwakarma, A., & Gupta, K. J. (2017). Isolation and structural studies of mitochondria from pea roots. In Gupta K. J. (eds) Plant respiration and internal oxygen: Methods and Protocols. 1 ed. pp.87-95.

Wada, H., Shackel, K. A., & Matthews, M. A. (2008). Fruit ripening in *Vitis vinifera*: apoplastic solute accumulation accounts for pre-veraison turgor loss in berries. Planta, 227, 1351-1361.

Wu, X., Jiang, L., Yu, M., An, X., Ma, R., & Yu, Z. (2016). Proteomic analysis of changes in mitochondrial protein expression during peach fruit ripening and senescence. Journal of Proteomics, 147, 197-211.

Xiao, Z., Liao, S., Rogiers, S. Y., Sadras, V. O., & Tyerman, S. D. (2018a). Effect of water stress and elevated temperature on hypoxia and cell death in the mesocarp of Shiraz berries. Australian Journal of Grape and Wine Research, 24(4), 487-497.

Xiao, Z., Rogiers, S. Y., Sadras, V. O., & Tyerman, S. D. (2018b). Hypoxia in grape berries: the role of seed respiration and lenticels on the berry pedicel and the possible link to cell death. Journal of Experimental Botany, 69(8), 2071-2083.

Zhang, X. Y., Wang, X. L., Wang, X. F., Xia, G. H., Pan, Q. H., Fan, R. C., ... & Zhang, D. P. (2006). A shift of phloem unloading from symplasmic to apoplasmic

pathway is involved in developmental onset of ripening in grape berry. Plant Physiology, 142(1), 220-232.

Zhang, Y., & Keller, M. (2017). Discharge of surplus phloem water may be required for normal grape ripening. Journal of Experimental Botany, 68(3), 585-595.